Electronic Supplementary Material (ESI) for Physical Chemistry Chemical Physics.


# Supplementary Material

# Mechanism research reveals the role of $Fe_n$ ($n = 2-5$) supported $C_2N$ as single-cluster catalysts (SCCs) for the non-oxidative propane dehydrogenation in the optimization of catalytic performance

Yu Zhang[a], Qin Chen[a] and Hui Zhang[a,*]

[a] *Center for Computational Chemistry and Molecular Simulation, College of Chemistry and Chemical Engineering, Southwest Petroleum University, Chengdu 610500, China*

[*]Corresponding authors.
*E-mail addresses:* huizhang@swpu.edu.cn (H. Zhang)

**Table S1.** Total Mulliken charge of $Fe_n$ cluster supported on $C_2N$

| Type | Line | Triangle | Tetrahedron | Butterfly | Square pyramid | Triangular bipyramid |
|---|---|---|---|---|---|---|
| Charge (\|e\|) | 1.157 | 1.144 | 1.341 | 1.172 | 1.461 | 1.134 |

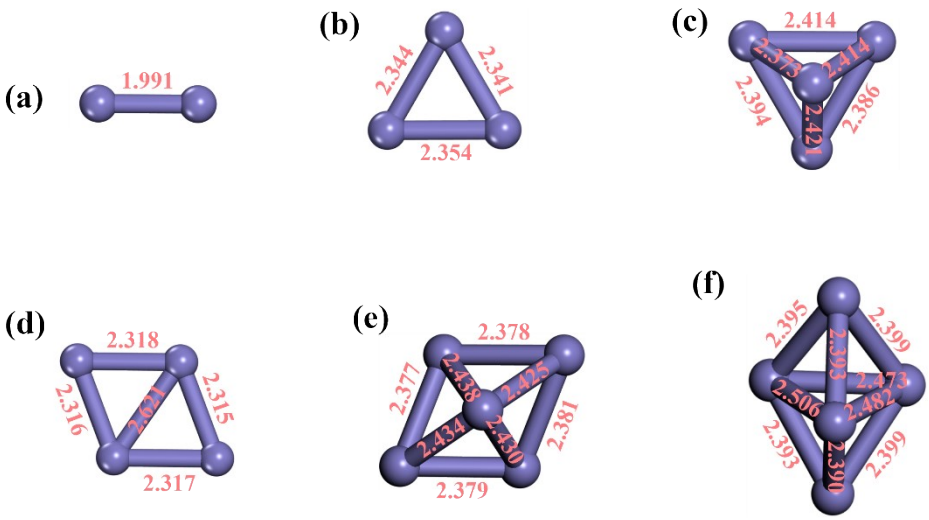


**Fig. S1** Optimized structures of pure $Fe_n$ clusters, and the bond lengths (Å) of Fe-Fe bonds in each $Fe_n$ cluster are also marked.

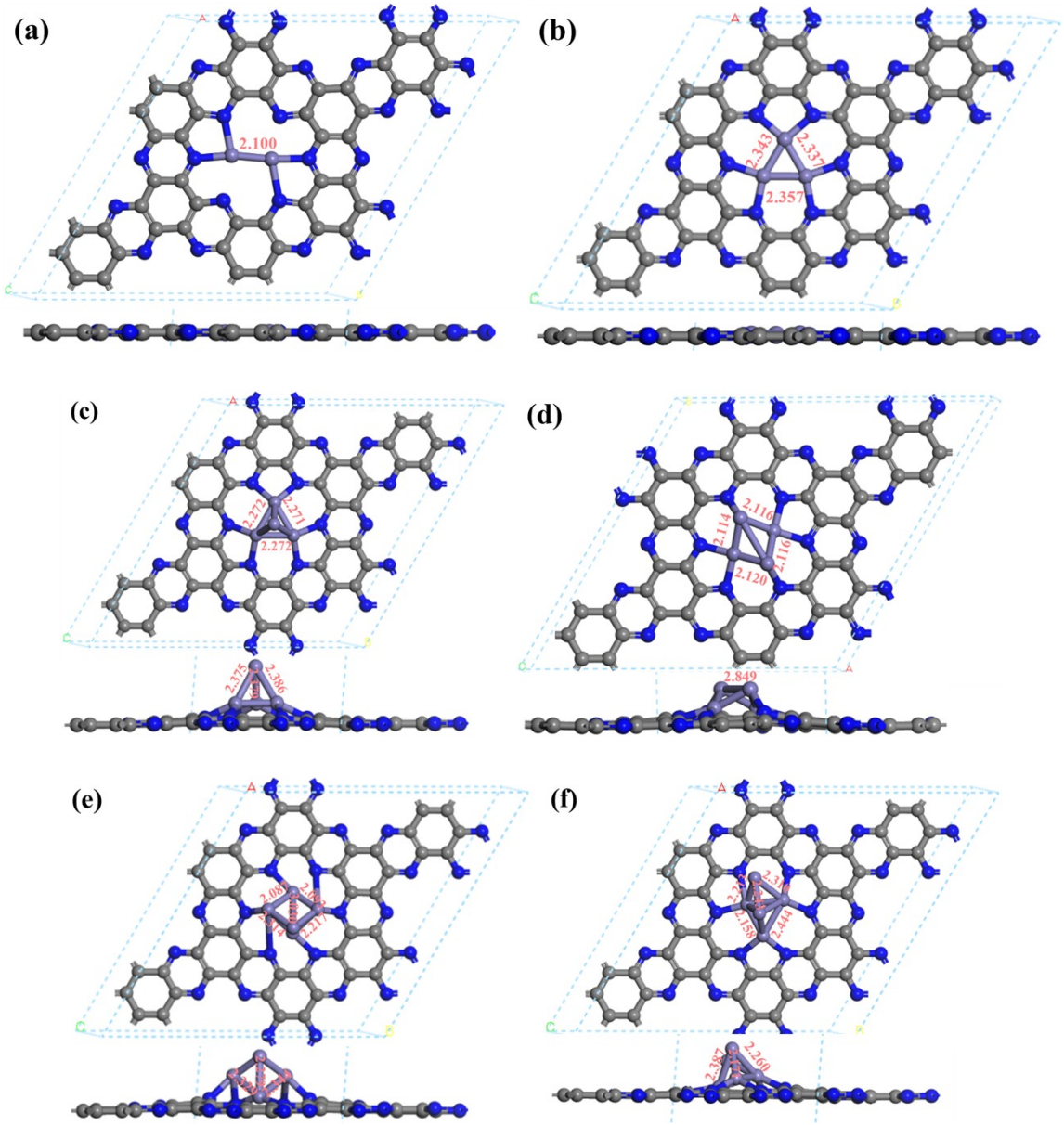


**Fig. S2** Top and side views of optimized structures of (a) $Fe_2$-$C_2N$, (b) $Fe_3$-$C_2N$, (c) $Fe_4$-$C_2N$ (tetrahedron), (d) $Fe_4$-$C_2N$ (butterfly-like), (e) $Fe_5$-$C_2N$ (square pyramid), and (f) $Fe_5$-$C_2N$ (triangular bipyramid). The bond length between two adjacent Fe atoms is marked in red font.

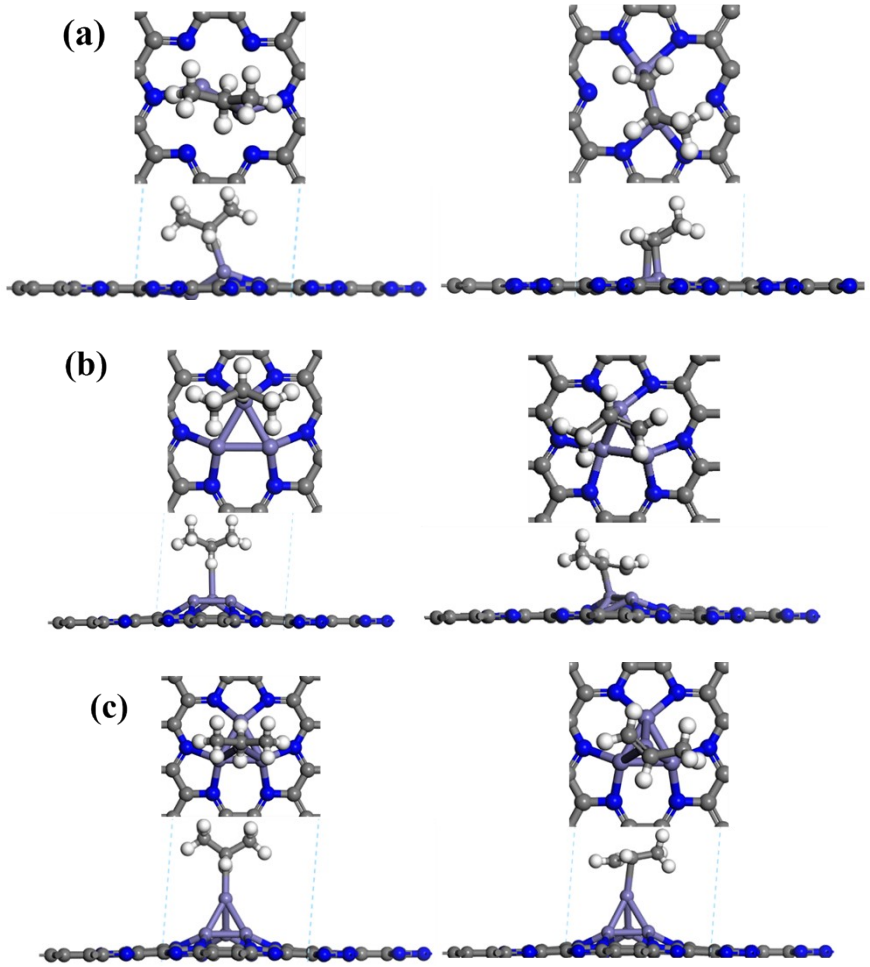


**Fig. S3** The top and side views of stable adsorption configurations of propane (left) and propylene (right) on (a)$Fe_2$-$C_2N$, (b)$Fe_3$-$C_2N$ and (c)$Fe_4$-$C_2N$ accordingly.

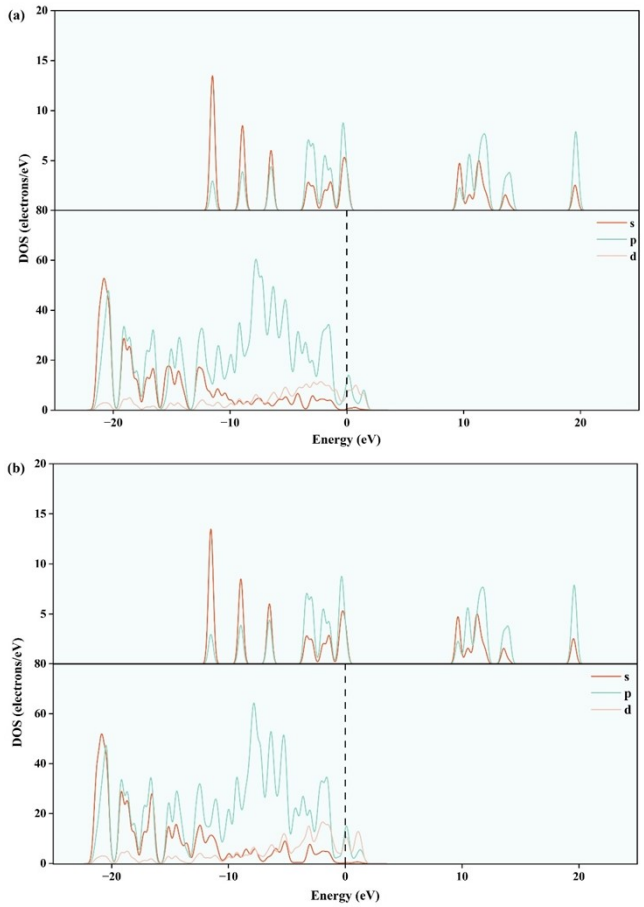


**Fig. S4** Density of states (DOS) of propane adsorbed on (a) $Fe_3$-$C_2N$ and (b) $Fe_4$-$C_2N$. The upper part of each image shows the orbitals of the free propane.

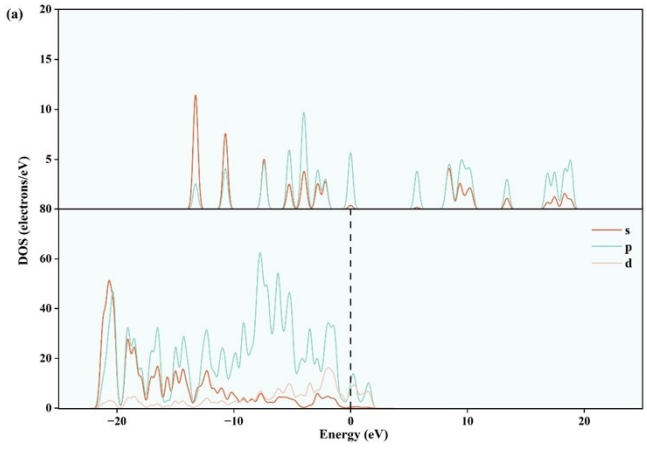

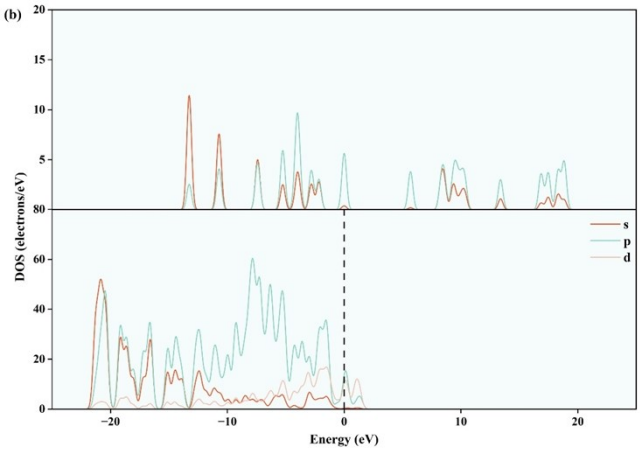


**Fig. S5** Density of states (DOS) of propylene adsorbed on (a) $Fe_3$-$C_2N$ and (b) $Fe_4$-$C_2N$. The upper part of each image shows the orbitals of the free propylene.

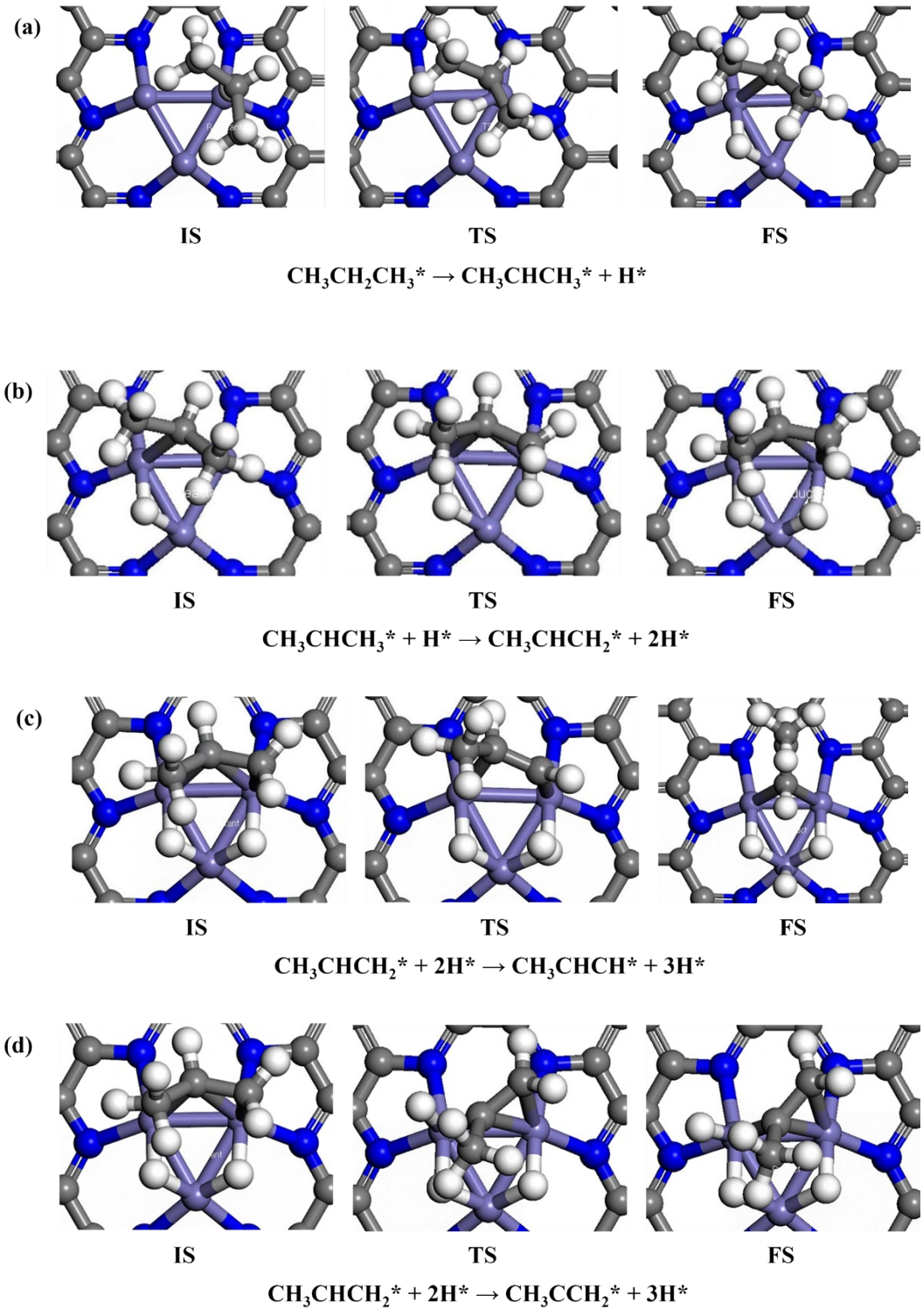


**Fig. S6** Optimized configurations of IS, TS, and FS on $Fe_3$-$C_2N$ along the route I.

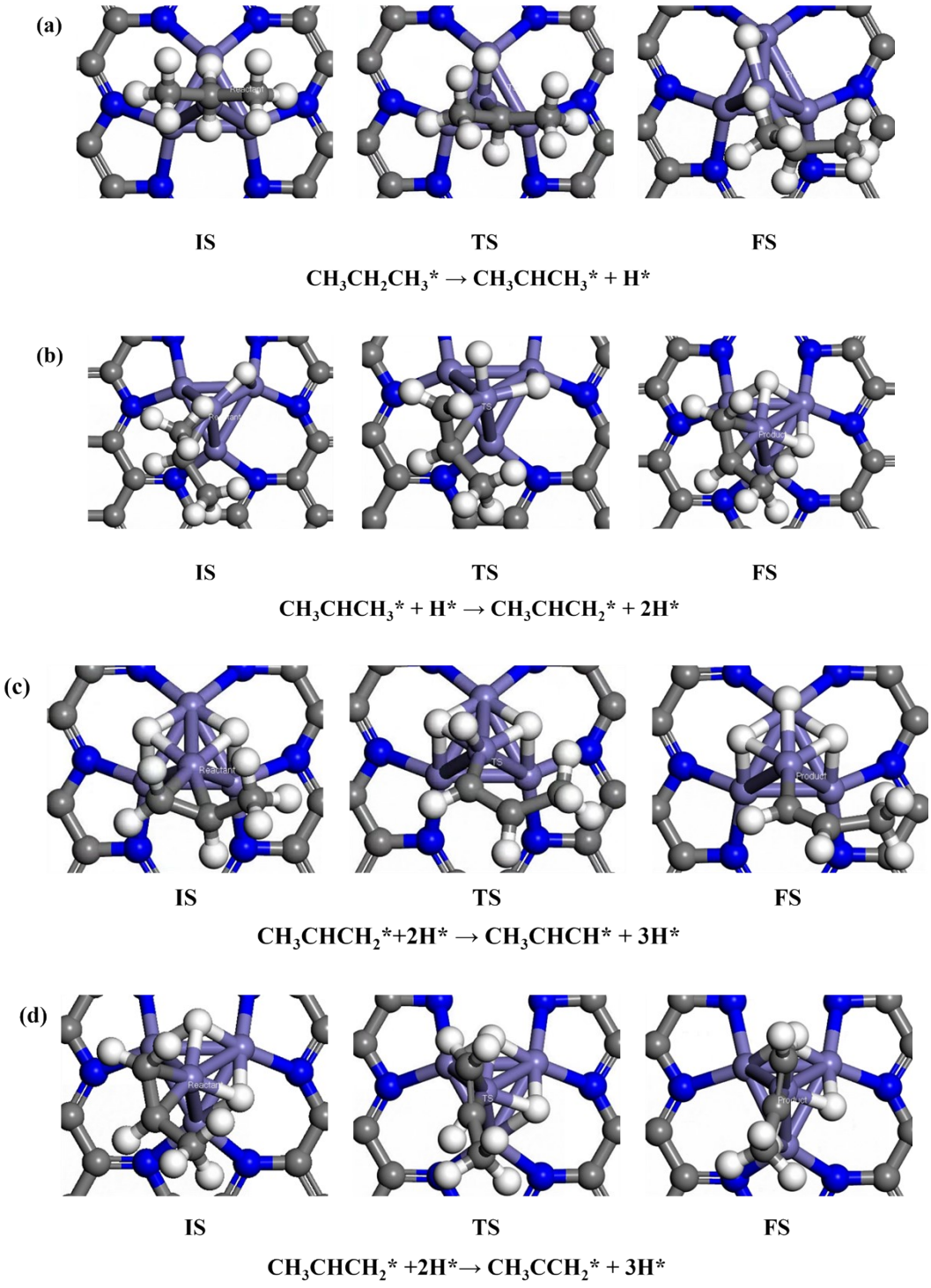


**Fig. S7** Optimized configurations of IS, TS, and FS on $Fe_4$-$C_2N$ along the route I.

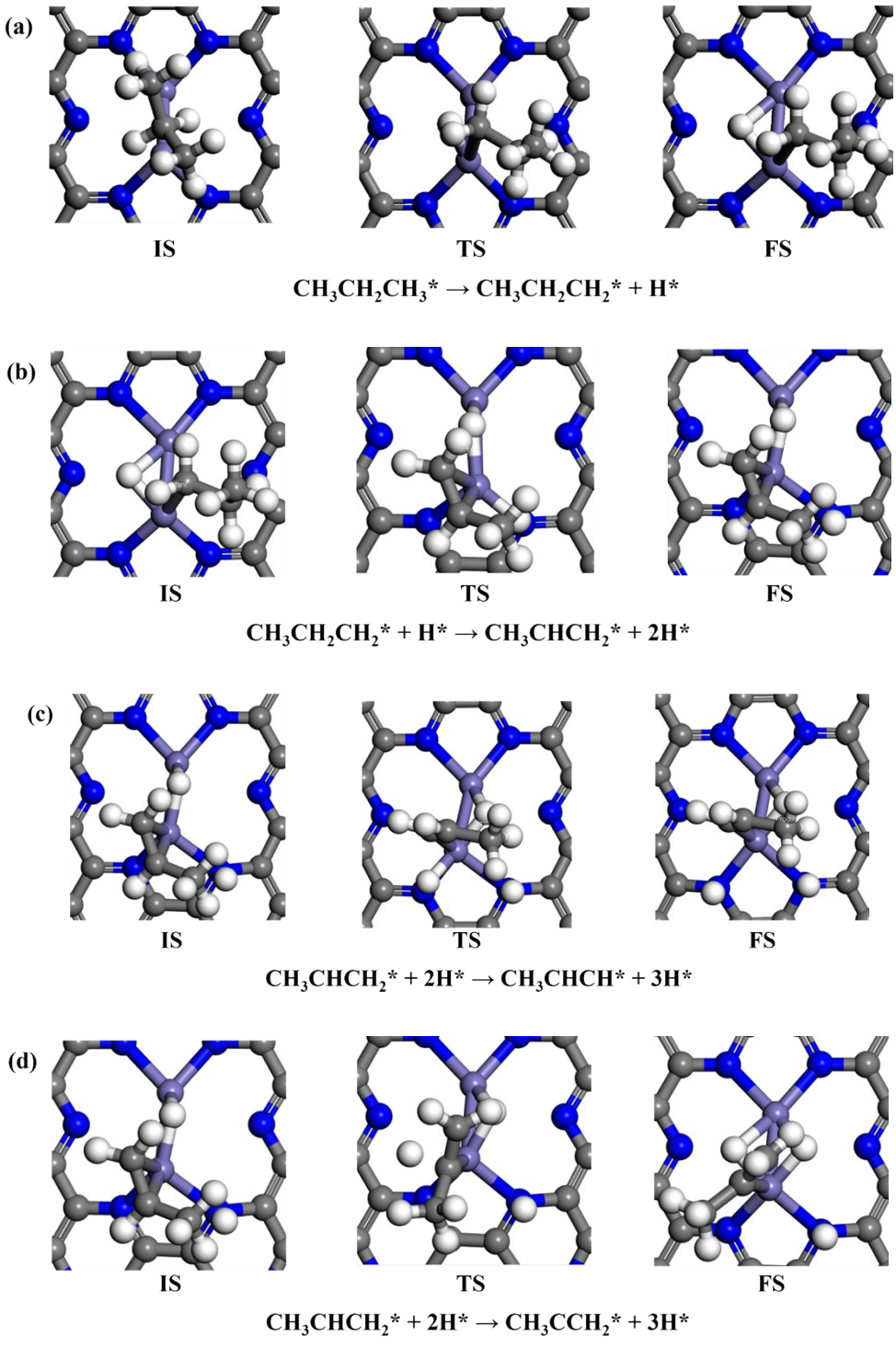


**Fig. S8** Optimized configurations of IS, TS, and FS on $Fe_2$-$C_2N$ along the route II.

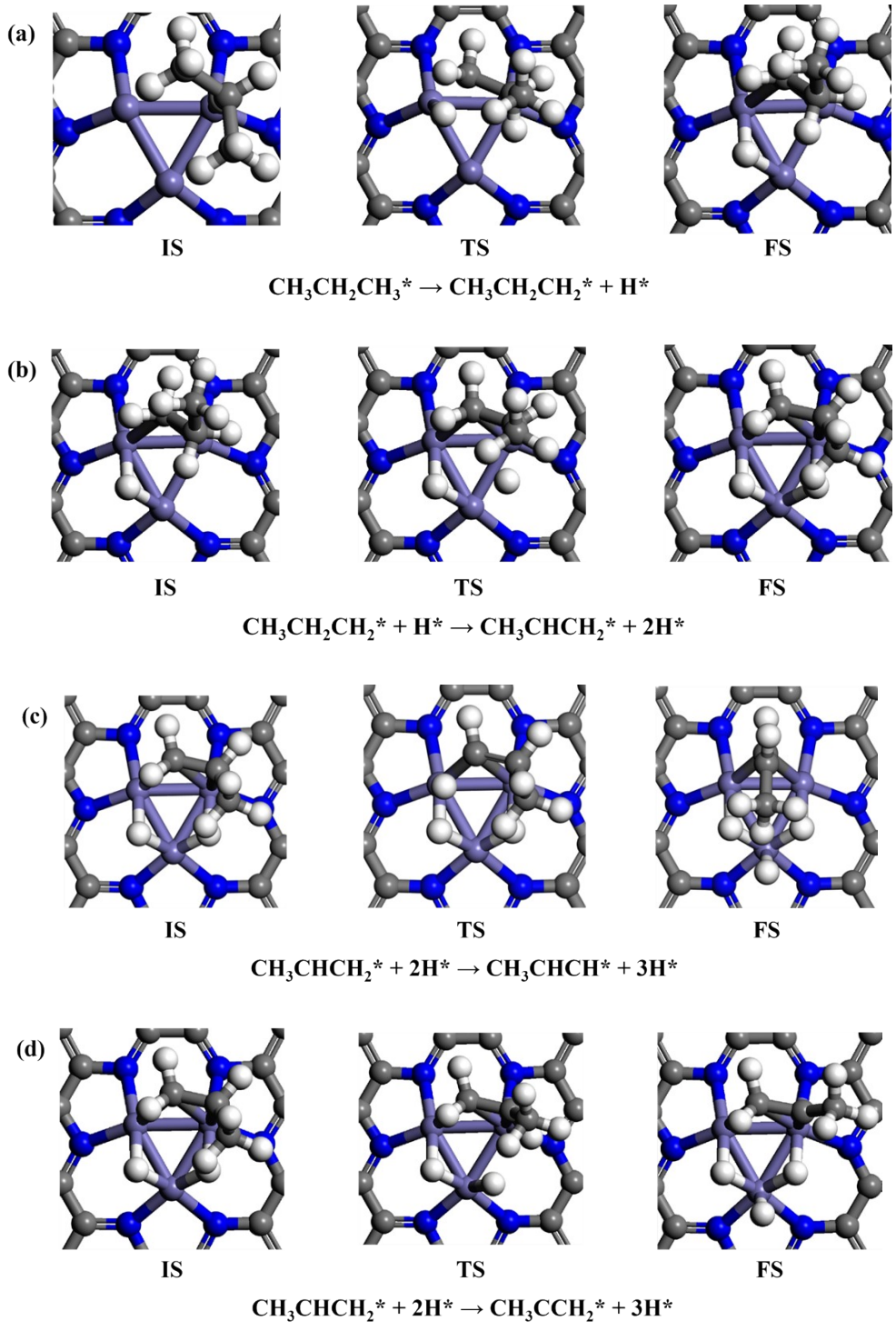


**Fig. S9** Optimized configurations of IS, TS, and FS on $Fe_3$-$C_2N$ along the route II.

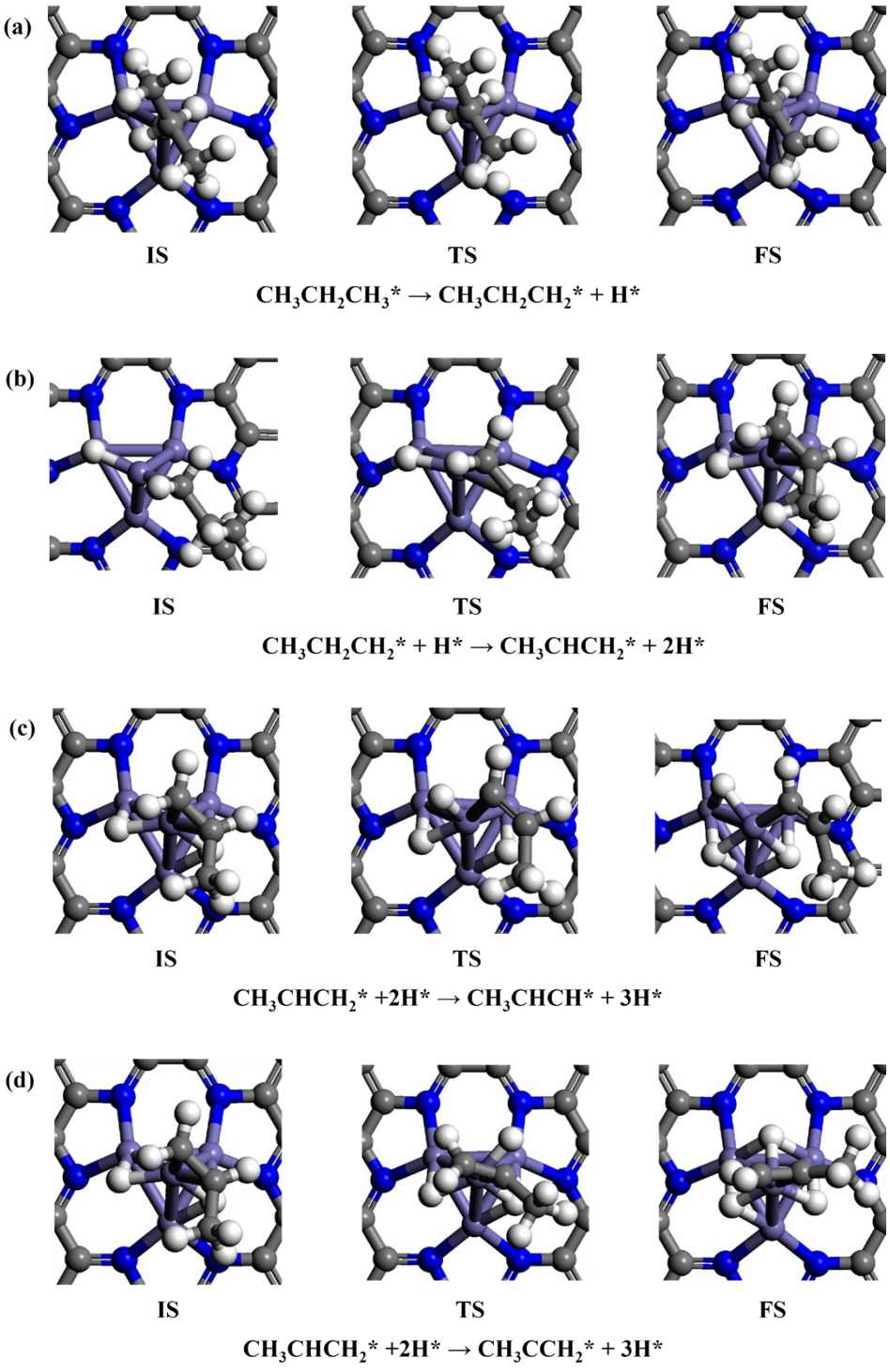


**Fig. S10** Optimized configurations of IS, TS, and FS on $Fe_4$-$C_2N$ along the route II.

(a)

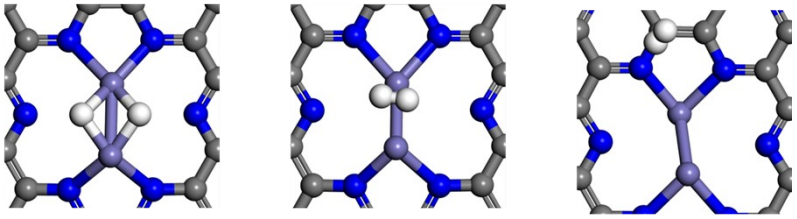

IS TS FS

$Fe_2$-(a): H*+H* → $H_2$

(b)

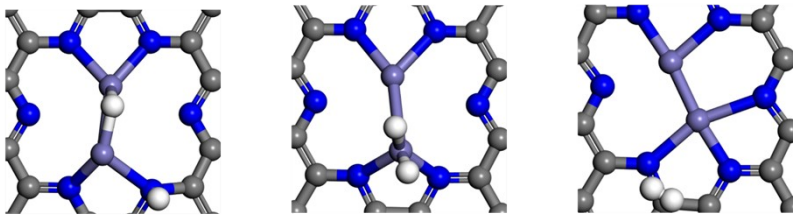

IS TS FS

$Fe_2$-(b): H*+H* → $H_2$

(c)

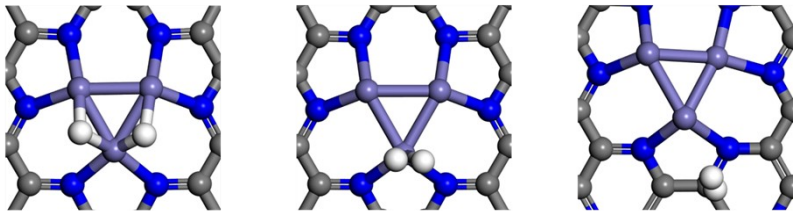

IS TS FS

$Fe_3$-(a): H*+H* → $H_2$

(d)

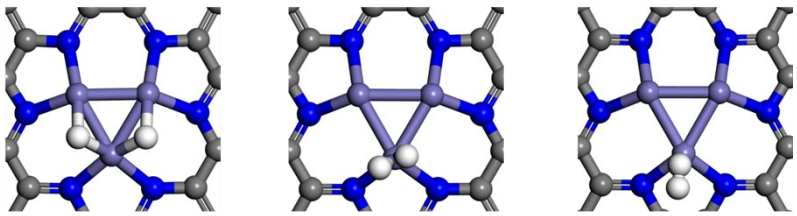

IS TS FS

$Fe_3$-(b): H*+H* → $H_2$

(e)

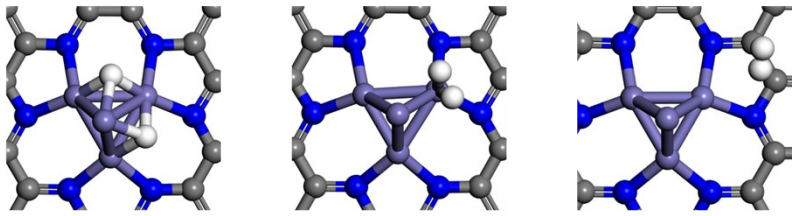

IS TS FS

$Fe_4$-(a): H*+H* → $H_2$

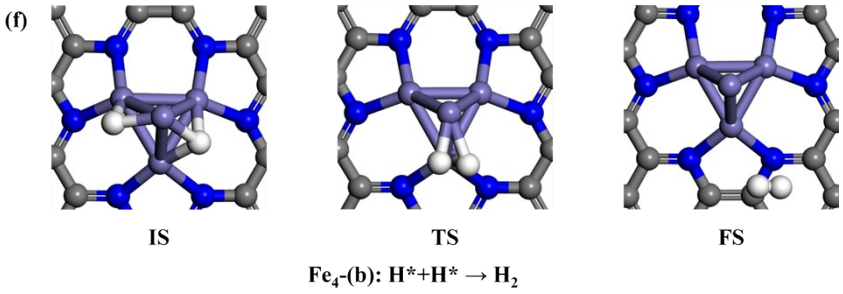


**Fig. S11** Optimized configurations of IS, TS, and FS to form $H_2$.